Title	A tribological study of double-walled and triple-walled carbon nanotube oscillators
Author(s)	Ma, Chi Chiu; Zhao, Yang; Yam, Chi Yung; Chen, Guan Hua; Jiang, Qing
Citation	Ma, C. C., Zhao, Y., Yam, C. Y., Chen, G. H., & Jiang, Q. (2005). A tribological study of double-walled and triple-walled carbon nanotube oscillators. Nanotechnology, 16(8).
Date	2005
URL	http://hdl.handle.net/10220/6778
Rights	©2005 Institute of PhysicsThis is the author created version of a work that has been peer reviewed and accepted for publication by Nanotechnology, Institute of Physics. It incorporates referee's comments but changes resulting from the publishing process, such as copyediting, structural formatting, may not be reflected in this document. The published version is available at: [DOI: http://dx.doi.org/10.1088/0957-4484/16/8/046].

A tribological study of double-walled and triple-walled carbon nanotube oscillators

Chi-Chiu Ma[1], Yang Zhao[1], Chi-Yung Yam[1], GuanHua Chen[1] and Qing Jiang[2]

1 Department of Chemistry, University of Hong Kong, Hong Kong ,People's Republic of China

2 Department of Mechanical Engineering, University of California, Riverside, CA 92521, USA

E-mail: ghc@everest.hku.hk and qjiang@engr.ucr.edu

Abstract

We reported in a previous study (Zhao *et al* 2003 *Phys. Rev. Lett.* **91** 75504) that energy transfer from the orderly intertube translational oscillation to intratube vibrational modes for an isolated system of two coaxial carbon nanotubes at low temperatures takes place primarily via two distinct types of collective motion of the carbon nanotubes, i.e., off-axial rocking motion of the inner tube and radial wavy motion of the outer tube, and that these types of motion may or may not occur for such a system, depending upon the amount of the initial extrusion of the inner tube out of the outer tube. Our present study, using micro-canonical molecular dynamics (MD), indicates the existence of an energy threshold, largely independent of system sizes and configurations, for a double-walled nano-oscillator to deviate from the intertube translational oscillation and thus to encounter significant intertube friction. The frictional forces associated with several distinct dissipative mechanisms are all found to exhibit no proportional dependence upon the normal force between the two surfaces in relative sliding, contrary to the conventional understanding resulting from tribological studies of macroscopic systems. Furthermore, simulation has been performed at different initial temperatures, revealing a strong temperature dependence of friction in the early phase of oscillation. Finally, our studies of three-walled nano-oscillators show that an initial extrusion of the middle tube can cause inner-tube off-axial instabilities, leading to strong frictional effects.

1. Introduction

Ever since their inception [1], carbon nanotubes (CNTs) have attracted a tremendous amount of experimental and theoretical interest. Synthesis of large quantities of CNTs [2] has been achieved through carbon-arc vapourization in a gas atmosphere or through transition-metal catalytic reaction. The latter method has been used to synthesize single-wall nanotubes

(SWNTs) [3, 4]. One can view a CNT as a rolled-up graphite sheet which is characterized by its chiral vector (*m, n*) [5, 6]. A huge variety of applications has been found for CNTs, such as single-electron transistors [7], tunnelling-magnetoresistance devices [8], CNT diodes [9], intramolecular junctions [10], molecular bearings [11, 12], springs [13], hooks [14], and oscillators [15–19], among which a promising aspect for nanotube applications is the emerging field of nanoelectromechanical systems (NEMS) [20]. The goal of high mechanical frequency in NEMS devices requires that actuators are very small, stiff, and structurally free of defects. Various types of molecular devices based on carbon nanotubes have been proposed, and most recently, Zheng and Jiang [15] have estimated that carbon nanotube mechanical oscillators can have frequencies far beyond one gigahertz, pointing to a path for creating various NEMS operating in the gigahertz range, which has been viewed as one of the milestones in the roadmap of molecular manufacturing [21, 22]. These devices will also serve as nanolabs for fundamental investigations into physics of the mesoscale.

Despite unlimited prospects of applications for low-friction nanobearings, nanosprings, and nano-oscillators, the performance, wear and load-bearing properties of fundamental components of these nanomachines are largely not understood. In particular, frictional properties of nanobearings and nano-oscillators demand much theoretical attention. The friction phenomenon is in general taken to denote the conversion of orderly translational energies into disorderly vibrational energies when two contacting parties slide with respect to each other. A system is called frictionless if the orderly translational energies remain constant over an extended period of time. Whether or not many traditional understandings of the friction phenomenon remain true for nanoscale machinery is an intriguing question. Nanoscale machinery creates an entirely new circumstance under which the concept of friction will be redefined. Cumings and Zettl report from their measurements that intertube static (dynamic) friction forces in multi-walled carbon nanotubes are less than 2.3 $(1.5)\times10^{-14}$ N/atom [13], while recent atomic-scale frictional force measurements on conventional materials yield values of frictional forces three orders of magnitude greater [23]. In a study of sliding between nested shells of multi-walled carbon nanotubes [24] Yu *et al* estimated a frictional force of 1.4×10^{-15} N/atom by pulling an inner tube out of an outer nanotube extremely slowly.

In a previous study [16], we reported that energy transfer from the orderly intertube axial oscillation to intratube vibrational modes for an isolated system of two coaxial carbon nanotubes occurs through two distinct forms of nanotube collective motion, i.e., the off-axial rocking motion of the inner tube and the radial wavy motion of the outer tube, and that the occurrence of such motion depends upon the amount of the initial extrusion of the inner tube. However, many issues remain unresolved. For instance, simulations in [16] were carried out at an initial temperature of 0 K, which leaves room for questioning what to happen if initially the oscillator is heated up to room temperature. It was found that the rocking or wavy motion occurs only when the initial extrusion length exceeds a threshold which varies from one oscillator to another. A natural question that emerges is whether there exists a universal threshold, perhaps in terms of energy per carbon atom. Lastly, the wavy motion leads to large friction. Can its occurrence be suppressed in a multi-walled oscillator resulting in much smaller friction?

It is the purpose of this work to build a comprehensive understanding of nanoscale motion-induced heating mechanisms in nano-oscillators, to explore various oscillator configurations other than open-ended double-walled carbon nanotubes (DWNTs), and to propose means for reducing heating and frictional effects that hinder oscillator performance and efficiency. Using

micro-canonical molecular dynamics, we will reveal the existence of an energy threshold, largely independent of system sizes and configurations, for a double-walled nano-oscillator to deviate from smooth intertube axial oscillation and thus to encounter significant intertube friction. Additional off-axial instabilities will be explored for one-end-closed DWNT oscillators and concentric triple-walled nanotube (TWNT) oscillators. In particular, TWNT axial oscillations are found to be unstable when the middle tube is extruded between the outer and inner tubes, and subsequent oscillations see the inner tube tilted towards the outer tube wall upon off-axial disturbance, causing a great increase in friction. The effect of pre-oscillation heating on the oscillator tribological properties will also be examined. Simulation will be performed at different initial temperatures revealing a strong temperature dependence of friction in the early phase of oscillation. In the absence of the wavy motion, the frictional force increases monotonically with the pre-simulation heating temperature of DWNT oscillators, but such a picture fails when the wavy motion dominates the energy-transfer process.

The friction phenomenon in nano-oscillators represents a more general problem of transfer of energies from the orderly degrees of freedom in a nanostructure into disorderly phonons, which may constitute an important step in equipartition and evolution towards statistical ergodicity. The collective motion that underlies the nanoscale friction phenomenon may manifest itself in new forms under various other circumstances (such as the nanosprings [11]), but the fact remains that the transfer channels are facilitated by collective modes in the nanosystems in the process of moving energies into disorderly phonons. It is also our intention to explore these issues further in this work.

In section 2 nano-oscillator configurations and simulation methods are described, and the relative kinetic energy is introduced as an indicator of the friction-induced heat transfer and a measure of the intratube temperature. In section 3 simulation results are given for various DWNT oscillators and their dissipative mechanisms. In section 4 TWNT oscillators are examined for novel mechanisms of energy dissipation. The effects of pre-oscillation heating on DWNT tribological properties are studied in section 5. Discussions are presented in section 6.

2. Methodology

The DWNT construct of the nanotube oscillator, as first proposed by Zheng and Jiang, is one of the most elementary realizations of a nanoscale oscillatory device. Five types of DWNT oscillators of various sizes are constructed together with a TWNT oscillator. Configurational details of the six oscillators are described in table 1, and illustrative examples of capped and uncapped DWNT oscillators are displayed in figure 1. All the DWNT oscillators have (5, 0) and (8, 8) nanotubes as the inner and outer tubes, respectively. This incommensurate pair is selected because incommensurate DWNTs are predicted to have corrugation against intertube sliding that does not increase drastically with system size, although in reality carbon atoms are likely to adjust positions locally to induce a weak length dependency of corrugation [18, 25–30]. For TWNT oscillators, we choose (5, 0), (8, 8) and (13, 13) carbon nanotubes as the inner, middle and outer tubes, respectively. All the inner nanotubes have both ends capped, while except for two configurations the outer nanotubes have both ends uncapped so that extrusion of the inner tube is possible at both ends. The only exception is a case for comparison, in which we have outer nanotubes with one end capped

and one end open. The intertube distance is ~3.4 Å, which is also the spacing between the adjacent sheets of graphite. The CHARMM force field is being used for both geometry optimization and molecular dynamics simulation of all the oscillators [31]. Geometry optimization is performed with the method of steepest descent.

At the beginning of the simulation, $t = 0$, the inner tube is pulled out of the outer tube along their common axis. A portion of the inner tube is thus exposed, the length of which at the beginning of the simulation is defined as the initial extrusion length s. The inner tube is then released with zero initial speed. A time step of 1 fs is used in the MD simulation. Instead of monitoring the system potential energy or the oscillation amplitude [17, 18], we focus on the phonon kinetic energies, i.e., the relative kinetic energy of two nanotubes, which is defined as

$$K_{\text{rel}}(t) \equiv \sum_i \tfrac{1}{2} m_i |\mathbf{v}_i^{\text{in}} - \mathbf{v}_{\text{ave}}^{\text{in}}|^2 + \sum_j \tfrac{1}{2} m_j |\mathbf{v}_j^{\text{out}} - \mathbf{v}_{\text{ave}}^{\text{out}}|^2 \quad (1)$$

where $\mathbf{v}_i^{in}$ $(\mathbf{v}_j^{out})$ and m_i (m_j) are the velocity and the mass of the ith (jth) atom in the inner (outer) tube, respectively; $\mathbf{v}_{ave}^{in}$ $(\mathbf{v}_{ave}^{out})$ is the average atomic speed of the inner (outer) tube. $K_{\text{rel}}(t)$ is a direct measure of the intratube temperature, i.e., an indicator of heat transfer from the orderly translational motion. It is chosen over other measures such as variations of the oscillation amplitudes because it provides a more accurate representation of the transfer dynamics for timescales shorter than the oscillator period. For an assembly of uncorrelated harmonic oscillators, the sum of their kinetic energies approximately equals that of potential energies. For low-energy oscillations in which the intratube motion of the carbon atoms is mostly harmonic with energies equally distributed into kinetic and potential portions, equation (1) is approximately one half of $E_{\text{loss}}(t)$, the combined loss of intertube potential energy and the orderly translational kinetic energy:

$$E_{\text{loss}}(t) \equiv E_{\text{tot}}(0) - [P_{\text{trans}}(t) + K_{\text{trans}}(t)] \quad (2)$$

where $E_{\text{tot}}(0)$ is the initial total system energy at $t = 0$, $P_{\text{trans}}(t)$ is the time-dependent potential energy between two nanotubes due to translational oscillation (while freezing the atoms in both nanotubes), and $K_{\text{trans}}(t)$ is the corresponding translational kinetic energy. $E_{\text{tot}}(0)$ is in fact the initial excess intertube van der Waals energy, which is set to zero if both nanotubes are kept still while sharing a common axis.

We carry out a series of simulations on the nanotube oscillators with various initial extrusion lengths s. Frictional forces incurred during the nanoscale oscillation are estimated, and their dependence on configurations and initial conditions of the oscillator is discussed.

3. DWNT oscillators

3.1. Rocking motion

Simulations are first performed for the case of the uncapped short-tube combination with two tubes of the same length 14.5 Å, as reported in [16]. For the purpose of discussion, calculated $K_{\text{rel}}(t)$ for this uncapped short-tube combination (14.5 Å/14.5 Å), which contains 294 atoms,

are again shown in figure 2(a) for four initial extrusion lengths s = 5, 10, 11, and 12 Å. For the largest initial extrusion length among the four, s = 12 Å, the corresponding centre-of-mass displacements of the inner and outer nanotubes perpendicular to translational direction are shown in figure 2(b). For s = 12 Å, about 0.17 eV of energy is transferred into $K_{rel}(t)$ within an initial 5 ps, and the inner tube then follows a stable axial trajectory as shown in inset (A) of figure 2(a). During the time period from the 20th to the 40th picosecond, the system undergoes rocking motion (cf inset (B) of figure 2(a)) [16], in which the phonons acquire a large portion of the initial energy from the translational degree of freedom. This rather surprising finding may have significant implications for the construction of nano-mechanical devices, and a close examination is thus warranted. At t = 500 ps, the DWNT oscillator with an initial extrusion length of s = 12 Å (11 Å) has an intratube temperature of 26.3 K (19.8 K), which is calculated from the relative kinetic energy $K_{rel}(t)$ *at* t = 500 ps.

As shown in figure 2(b), the onset of the rocking motion is correlated with a drastic change in intertube radial movements which occur between 20th and 40th picosecond from the start of the simulation. The rocking motion introduces radial movements of the inner tube with respect to the outer tube, and thus excites a large number of phonons in the system. This rocking motion instability, however, is self-mitigating, as it creates phonons and reduces the overall amplitude of the radial movements. These negative feedbacks suppress the rocking motion, and correspondingly, the DWNT oscillator reaches a new quasi-equilibrium in which intertube radial motion dissipates completely into thermal vibrations (cf inset (C) of figure 2(a)). It is remarkable that such a quasi-equilibrium can be sustained for a long time with relatively few frictional effects between the nanotubes.

The frictional force per carbon atom can be estimated from the energy dissipation rate. For an initial extrusion length s =12 Å, the average velocity of the inner tube from t =150 to 500 ps is 1.4 Å ps^{-1}. The energy dissipation rate, $\Delta E_{loss}/\Delta t$, is roughly twice the rate of increase of the relative kinetic energy, $\Delta K_{rel}/\Delta t$. From figure 2(a), $\Delta K_{rel}/\Delta t$ can be calculated from $K_{rel}(t)$ averaged over 5 ps. Consequently, the average frictional force estimated for the time period from t =150 to 500 ps is approximately 2×10^{-15} N/atom. If the dissipative strength from t = 300 to 500 ps is to be maintained, the translational motion of the DWNT oscillator will be brought to a full stop at t =2 ns.

Similar dissipation mechanisms via an off-axial rocking motion are also found in a different oscillator configuration in which the outer tube has one end capped and the other end open (the inner tube has both ends capped). However, for the capped short-tube combination, frictional hindrance to the translational oscillation is augmented by an additional dissipation mechanism pertaining to the abrupt reversals of the inner tube at the capped end of the outershell, which, standing alone, delivers a frictional effect comparable in strength to that for the uncapped short-tube combination. The DWNT oscillator undergoes an initial energy optimization with the capped ends of the two nanotubes separated by about 3.4 Å prior to simulation. Calculated $K_{rel}(t)$ with s =10, 11 and 12 Å for the capped short-tube combination are shown in figure 3(a), and for s =12 Å the centre-of-mass displacements of the inner and outer nanotubes along and perpendicular to translational direction are shown in figures 3(b) and (c), respectively. Analogous to the uncapped short-tube combination, about 0.17 eV is transferred into $K_{rel}(t)$ within the initial 3 ps for the capped short-tube combination with s =12 Å. The onset of the rocking motion also correlates with the drastic increase in intertube radial movements between the 20th and 40th picosecond from the start of the simulation, as shown in figure 3(c). The capped oscillator with s =10 Å continues the translational motion with negligible frictional effects, while for s =11 Å, an increase of $K_{rel}(t)$

induced by the rocking motion happens after 80 ps, as shown in figure 3(a). In capped nanotubes, however, there are abrupt reversals of the inner tube as it bounces off the capped end of the outershell. The reversals are represented by the spikes in K_{rel} in figure 3(a), revealing that the reversals are mostly elastic collisions. At the same time, it should be pointed out that there is an inelastic portion of the collisions that underlies the new dissipation mechanism in addition to that via the rocking motion. Upon each collision a small percentage of the energies that show up in K_{rel} (as represented by the spikes) does not return to the translational oscillation. Those spikes are especially long-lived for s =10 Å, as the fluctuations in K_{rel} for that case, thanks to the absence of any additional disturbance aside from the initial residue intertube interactions, actually decrease with time in contrast to the other two cases in figure 3(a). Due to the impact incurred when the inner tube reverses directions at the capped sleeve end, the rate of decay of the translational energies from t =150 to 500 ps is found to be twice as large as that with uncapped oscillators under similar conditions, implying that the collisional dissipation doubles the amount of frictional effects. It follows that the frictional force per atom for the capped oscillator is also about twice as large. It has been estimated that translational oscillation will be fully dissipated at t =1.6 ns for an initial extrusion length of s = 12 Å.

3.2. Wavy motion

The DWNT systems discussed so far comprise relatively small-sized nanotubes with a few hundreds of atoms. To further explore the configurational cause of the frictional effects, we now examine DWNT oscillators of much larger sizes. For reasons that will become evident later, we first construct a mixed-tube combination in which the inner tube is 14.5 Å, and the outer tube, 70 Å. Calculated $K_{rel}(t)$ for the mixed-tube combination is shown in figure 4(a) for s =12.25 Å, and the centre-of-mass displacements of the inner and outer tubes along the axial direction, and in a radial direction, are shown in figures 4(b) and (c), respectively. A leap of the phonon kinetic energies, preceded by rocking motion, is found to take place about 300ps after the start of the simulation. The occurrence of the rocking motion coincides with the onset of large intertube radial movements (cf figure 4(c)), and a significant slowdown in translational oscillation (cf figure 4(b)). The latter is attributed to the non-coaxial movements of the inner tube that rock inside a previously still outershell, and impede the otherwise smooth translational oscillation. At t =500 ps, the DWNT oscillator reaches an intratube temperature of 8.0 K.

We next focus on a long-tube combination in which the outer tube has a length of 70 Å, and the inner, 55 Å. There are altogether 1242 carbon atoms in the long-tube combination, which is about four times larger than the short-tube combination. Our simulations reveal that the translational motion for the long-tube combination is further damped when the length of the inner tube is longer than or comparable to the characteristic length scale of the outershell wavy motion, which is found to be around 30 Å. A demonstration of the outershell wavy motion is given in the inset of figure 5(a), and Fourier transforms of outershell carbon atom displacements in a direction perpendicular to the translational oscillation are plotted in figure 5, which shows that the predominant structure in the spectra is located at a wavevector no greater than about 0.21 Å $^{-1}$ corresponding to a characteristic length scale of 30 Å [16]. In comparison, for the case that the inner tube is much shorter, for example, 14.5 Å as in the mixed-tube combination, and thus it can move freely to adjust to the movements of the much longer outer tube, the translational motion is not damped by the wavy motion of the outer nanotube (cf figure 4(a)). The dependence of formation of wavy motion on initial

DWNT optimizations is studied, and results show that reversing the order of energy optimization and inner tube extrusion may alter the short-time dynamics of wavy motion, but it has no significant effect on its long-time frictional impedance against intertube oscillation. As shown previously [16], the dissipative effect of the rocking motion is overshadowed, in the long-tube combination, by that of the wavy motion, and the latter can be suppressed by selecting a short inner tube or by freezing the atoms of the outer tube.

An MD simulation for a much longer time (up to 2 ns) is performed for the long-tube combination with s =27.5 and 52.5 Å in order to arrive at a full picture of the heating process. Calculated $K_{rel(t)}$ for the long-tube combination with s =27.5 and 52.5 Å are plotted in figure 6(a), and the centreof-mass displacements of the inner and outer nanotubes along and perpendicular to translational direction for s =27.5 Å are shown in figures 6(b) and (c), respectively. The roughly linear increase of $K_{rel}(t)$ with time is sustained only for 500 ps (1500 ps) for s =27.5 Å (52.5 Å), and after that, the decrease in the translational oscillation amplitude levels off. This can be attributed to the disappearance of wavy motion when the translational oscillation with a shrinking amplitude is unable to deliver a fresh supply of energies to the wavy motion in the outer shell which is itself dissipating energies to more disorderly phonons. From this long-time behaviour of wavy motion, it appears that the translational energies are first dissipated into low-energy phonons such as the wavy motion which is to be distinguished from higher energy phonon modes. The dissipation process moves upwards across the spectrum. Such behaviour bears resemblance to thermal relaxation for harmonic systems (or systems with quadratic and quartic interparticle potentials) which involves a sequential decay of independent phonon modes starting with those of the lowest frequencies [32]. As time passes, eventually the higher energy phonon modes in the nanotubes are excited with energies transferred from the lower energy phonon modes, and that is when the wavy motion disappears and the slope change in K_{rel} occurs. For s =27.5 Å, no wavy pattern exists after the slope change in $K_{rel;}$ instead, disorderly movements of individual atoms are found to be much faster than the wavy motion, implying higher phonon energies. If the dissipative strength from t =1.7 to 2 ns is sustained after t =2 ns for s =27.5 Å, the oscillator will be brought to a full stop at about t = 40 ns. At t = 500 ps, the intratube temperature reaches 14.6 K (26.3 K) for an initial extrusion length s =27.5 Å (55.5 Å).

The frictional forces attributed to the wavy motion is significantly larger than those estimated previously for the short-tube combination. For the long-tube combination (70/55 Å) and s = 55.5 Å, the average velocity between 150 and 500 ps is 4.4 Å ps^{-1}, and the average frictional force is 1×10^{-14} N/atom, which is much higher than that estimated from the short-tube oscillator and s =12 Å. For s = 7.5 Å, no rocking or wavy motion is present. The decay rate of translational energies is about 400 times smaller than that for s = 55.5 Å, and the corresponding velocity is 2.2 Å ps^{-1}. The frictional force is then estimated to be 2×10^{-17} N/atom. Our estimates are not inconsistent with those of Cumings and Zettl [13], and of Yu *et al*. We note that Cumings and Zettl excluded the oscillatory motion in their estimates (i.e., no repeated movements of nanotubes were allowed prior to those friction force measurements, and therefore, phonon effects on the intertube friction could not be properly taken into account), and that the estimate of Yu *et al* was based upon a quasi-static process. Despite that, our estimates fall below those of Cumings and Zettl.

In traditional models of friction, the normal forces between two surfaces sliding with respect to each other determine the size of the microscopic contacting area, and consequently, the frictional forces between the two surfaces. For nano-oscillators, the conventional

connection between interlayer normal and frictional forces no longer exists. The normal forces between inner and outer tubes have been estimated from the intertube van der Waals energy as a function of the intertube spacing. The intertube van der Waals energy is the difference between the DWNT van der Waals energy and the sum of the van der Waals energies of isolated inner and outer nanotubes. The normal forces between inner and outer tubes are found to be 10^{-10} N/atom for the long-tube combination without the wavy motion, which is compared with the estimated frictional forces of the order 10^{-17} N/atom. The wavy motion only results in a slight increase in the averaged intertube normal forces (<5%) due to the fact that the intertube distance is beyond the repulsive wall defined as where the van der Waals potential rises steeply with decreasing intertube distance, although frictional forces in the presence of the wavy motion are significantly larger than those from other mechanisms (about two to three orders of magnitude larger). This brings us to the conclusion that for long-tube combinations significant friction only arises in the presence of wavy motion in the outer tube, and smooth, unperturbed surfaces sliding with respect to each other do not encounter friction that depends on the normal force in the traditional sense.

In comparison with the capped short-tube combination, a capped long-tube combination with a 70 Å outer tube and a 55 Å inner tube is constructed for simulation. The DWNT oscillator undergoes an energy optimization with the capped ends of the two nanotubes separated by about 3.4 Å prior to simulation. The initial extrusion length is set at s =27.5 Å. Calculated $K_{\mathrm{rel}}(t)$ is shown in figure 7(a) for a time period of 500 ps. After the innershell is telescoped out, the DWNT oscillator with a one-end-capped outershell appears to possess a large amount of residue interaction energies, the relaxation of which results in an immediate radialbreathing-mode-like vibration in the outershell as exhibited in the relatively large $K_{\mathrm{rel}}(t)$ for small t. Centre-of-mass displacements of two nanotubes along the axial direction and in a direction perpendicular to the axial direction are plotted in figures 7(b) and (c), respectively. The spikes in $K_{\mathrm{rel}}(t)$ correspond to the collisions between the capped ends of the two nanotube, and correspondingly, centre-of-mass displacements of the two reach points of extremum at those times. Because $K_{\mathrm{rel}}(t)$ shown is sampled every 50 fs, a few spikes are missed in the sampling in figure 7(a). As has been previously addressed for the capped short-tube combination, intertube collisions between two capped ends bring additional dissipation to the translational oscillation. The slope of $K_{\mathrm{rel}}(t)$ for up to t =400 ps is at least twice as steep as that for the uncapped case. As a result, the oscillator amplitude is quickly diminished, as shown in figure 7(b), and the energy source that feeds $K_{\mathrm{rel}}(t)$ exhausted. DWNT oscillators with capped outershells, therefore, differ significantly from those with uncapped outershells in their dissipation mechanisms. In addition to the frictional loss attributed to the wavy motion which also appears in the latter, the former surrender a large amount of translational energies to the intratube phonons during collisions between capped ends, which, in turn, may aid friction via wavy motion.

3.3. Energy threshold

An important quantity of interest is the threshold s_{c} of the initial extrusion length above which the rocking mode or the wavy motion kicks in and the oscillator encounters significant friction.

We first look at the energy threshold for the short-tube combination. As shown in figure 2(a), for s = 5 Å, no rocking motion appears in the oscillator made of two short nanotubes (14.5 Å /14.5 Å), and the system maintains translational oscillation with few frictional effects,

while for $s = 10$ Å, an increase of $K_{rel}(t)$ preceded by the rocking motion occurs after 380 ps. Further simulations with other values of s have been performed, and s_c is estimated to be between 5 and 6 Å, or about 35–40% of the total nanotube length, which corresponds to a threshold of 2.1–2.6 meV/atom in excess intertube van der Waals energies. Below this threshold s_c, the rocking motion (cf inset (B) of figure 2(a)) is energetically unfavourable, and is suppressed, leaving the oscillator in nearly frictionless motion from the start of oscillation, and above s_c, the initial metastable motion (cf inset (A) of figure 2(a)) is no longer stable with respect to the rocking motion due to the entropic effect.

Similar energy thresholds can be found for the long-tube combination (70 Å /55 Å). If the initial extrusion length does not exceed a certain value, for example, s =7.5 Å, our simulations show that the rocking motion of the inner tube does not occur, and neither does the wavy motion of the outer tube. As a result, the oscillation encounters virtually no heating, and is nearly frictionless. This can be explained by the absence of sufficient system energies to initiate the wavy motion in the outer nanotube for small initial extrusion lengths. For a slightly larger initial extrusion length s =11.5 Å, the oscillator experiences qualitatively more significant frictional effects which generate a significantly larger $K_{rel}(t)$ after 100 ps in comparison with the case of s =7.5 Å. From this we conclude that the threshold s_c for the long-tube combination should fall between 7.5 and 11.5 Å, i.e., about 14%–21% of the total inner tube length, which corresponds to a threshold of about 1.5–2.2 meV/atom in the excess intertube van der Waals energy. Despite the facts that the long-tube combination is about four times as large as the short-tube combination, and that mechanisms vary for significant acquisition of phonon energies in the two cases, the threshold energies per atom surprisingly do not differ much for the two configurations. This points to the similarity in the low-energy landscape despite varying system sizes.

4. TWNT oscillators

It is interesting to perform simulations on three-body TWNT oscillators as a comparison with those on DWNT oscillators. Not only are TWNTs closer to MWNTs commonly seen experimentally, but also TWNT oscillators may reveal novel energy dissipation mechanisms absent from DWNT ones. To our knowledge, this is the first time that TWNT oscillators are studied via molecular dynamics simulation without constraining movements of any atoms in the TWNT. Only one configuration is constructed with two long outershells of an equal length, 70 Å, and a short inner nanotube of 55 Å. Either the inner tube or the middle tube is initially extruded from their optimized configuration with three tubes sharing a common centre of mass.

In figure 8(a), $K_{rel}(t)$ is shown for a time period of 500 ps and an initial extrusion length of 55.5 Å for the inner nanotube. This means that the 55 Å nanotube is pulled out of the DWNT outershell entirely with a 0.5 Å spacing between them. This behaviour of $K_{rel}(t)$ is in close resemblance to that of the DWNT oscillators, implying that the underlying energy dissipation mechanism is also via wavy motion. Despite the doubling of the outershell mass in comparison to the DWNT oscillator, the effect of the wavy motion on translational oscillation does not appear to be suppressed. In the first 500 ps, K_{rel} gains about 3 eV, which is compared with a 2.5 eV increase of K_{rel} for the DWNT oscillator with s =55.5 Å [16]. Centre-of-mass displacements of three nanotubes along the translational direction are shown in figure 8(b). The two outer nanotubes display little relative motion, which may be attributed to the large corrugation effect between the commensurate armchair–armchair pair. The frictional force for the TWNT oscillator is estimated to be 10^{-14} N/atom, which is similar

to that of the DWNT oscillator with the same initial extrusion length.

In figure 9(a), $K_{rel}(t)$ is compared for two initial configurations of the TWNT oscillator: (1) the middle tube extruded, and (2) the inner tube extruded, with the same extrusion length $s = 35$ Å at $t = 0$. The extrusion-induced excess intertube van der Waals energy for the two cases are (1) 26.16 eV, and (2) 9.617 eV, respectively, at $t = 0$. The case of extruding the middle tube displays significantly larger frictional effects for reasons that will become clear later. Centre-of-mass displacements along the translational direction for the three tubes are shown in figure 9(b) for the case of extruding the middle tube at $t = 0$, and the corresponding centre-of-mass displacement of the inner tube in a radial direction, in figure 9(c). Upon middle-tube extrusion, the portion of the inner tube not covered by the middle tube is energetically unstable, and it is attracted to the side wall of the outer tube under slight deviations from its coaxial position (cf figure 10). Those off-axial deviations can be easily generated as the TWNT oscillator comes under motion-induced heating due to the intertube frictional effect. Once the middle tube is released, the three tubes oscillate out of phase with the inner tube experiencing significant radial movements (cf figure 9(c)). For comparison, centre-of-mass displacements along the translational direction for the three tubes are displayed in figure 9(d) for the case of extruding the inner tube with an initial extrusion length $s = 35$ Å (same extrusion length s as in figure 9(b)). The two outershells are approximately locked in phase similar to the behaviour in figure 8(a) (which is for a much larger inner-tube extrusion length $s = 55.5$ Å).

As previously mentioned, the large amplitude of the radial centre-of-mass movements of the inner tube in figure 9(c) is attributed to energetic instabilities of the coaxial configuration when the middle tube is vacated due to extrusion. Such energetic instabilities are absent in DWNT oscillators for which the intertube wall-to-wall distance remains at about 3.4 Å at all times. As demonstrated in figure 10, the intertube van der Waals energy of the inner and outer tubes in the absence of the middle tube reaches a minimum when the inner tube is displaced radially from its coaxial position by about 3 Å so that the intertube wall-to-wall distance is approximately 3.4 Å. This explains the drastic difference between radial movements of the inner tube in figure 9(c) (middle tube extruded) and figure 9(e) (inner tube extruded). If initially the middle tube is extruded, during the subsequent oscillations, the portion of the inner tube not covered by the middle tube will tilt towards the side wall of the outer tube, hindering the translational movements of the three tubes and causing large intertube friction, as reflected in figure 9(a). Analogy can be made between this off-axial behaviour of the inner tube and the rocking motion in DWNT oscillators, although the latter is caused by entropic effects.

Despite their relative simplicity, nanomechanics of TWNTs, compared with those of DWNTs, give a better description of general MWNT performance in various nanomechanic configurations, such as oscillators, bearings, and other sword-and-sheath pairings. Therefore, TWNT energetic instabilities discussed here may have important implications to MWNT-based nanodevices that go well beyond the gigahertz oscillators.

5. Temperature effect

So far, simulations on the DWNT/TWNT oscillators have been performed here with a micro-canonical ensemble, which differs from a number of other simulations on DWNT oscillators [17–19, 33]. For example, Legoas *et al* run simulations with a canonical

ensemble for a variety of temperatures up to 400 K, and Rivera *et al*, for a temperature range from 275 to 450 K [17, 18]. Guo *et al* thermally equilibrate DWNT oscillators with a bath to reach an initial temperature, then switch to a micro-canonical ensemble for simulations, and a similar approach is used by Servantie and Gaspard fixing the initial temperature at 300 K [19, 33]. Translational oscillations of the DWNT excite a number of phonons [34, 35], some of which may have a relatively long lifespan despite the nonlinear nature of the intertube and intratube interactions. By adopting the canonical ensemble from the start of the simulation, certain collective phenomena, such as the wavy motion of the outershell, may be sidestepped by the random thermal agitation imposed. Our simulations so far have been carried out at much lower temperatures than those used by other authors [17–19, 33].

Here we take a similar approach to that of Guo *et al*, and that of Servantie and Gaspard [19, 33], to investigate the temperature effect on the frictional behaviour of DWNT oscillators. The long-tube combination (55/70 Å) is adopted, and the DWNT oscillator is initially heated up to various temperatures (0, 20, 60, 120, 180, and 240 K) before commencing simulations in a micro-canonical ensemble. Two initial inner-tube extrusion lengths are used, s =7.5 and 27.5 Å. The relative displacement between the centres of mass of the inner and outer nanotubes is plotted as a function of time in figure 11 for the $s = 27.5$ Å case. The zero-temperature simulation has already been discussed in length in section 3. The apparent slowdown of the oscillation-amplitude depreciation at about $t = 500$ ps is attributed to the disappearance of the wavy motion in the DWNT. As the oscillator is pre-heated to 60K, the duration of the wavy motion is shortened to about 150 ps, and as a result, the slope change in the amplitude envelope happens much earlier than in the zero-temperature case. Due to combined frictional effects from the wavy motion and the pre-heating-induced thermal roughness, much greater energy dissipation is found for the DWNT oscillator in the initial phase of the oscillation. Further increases in the pre-heating temperature lead to much larger initial friction and faster disappearance of the wavy motion, as demonstrated in the lower three panels of figure 11. When the DWNT is pre-heated to 240 K, the oscillation amplitude is diminished entirely within 400 ps.

Frictional forces per atom for $s = 7.5$ Å have been estimated, and plotted as a function of initial DNWT temperatures in figure 12. The estimated frictional force per atom is found to increase monotonically with the initial DWNT temperature, and varies by about one order of magnitude as the initial temperature is increased from 20 to 180K. This indicates that, for $s = 7.5$ Å, the frictional force is predominantly caused by random thermal roughness of contacting surfaces created either by pre-simulation heating or motion-induced self-heating. Such a behaviour is in qualitative agreement with findings by Servantie and Gaspard [33], which showed that the dynamic friction coefficient increases linearly with the temperature. In figure 12, the dependence of the frictional force per atom f on the pre-heating temperature T is given a linear fit:

$$f \approx 0.12T \tag{3}$$

where f is in units of 10^{-16} N/atom, and T is in units of kelvin. Much attention has also been paid to the temperature dependence of the quality factor Q in micro- and nanoscale mechanical structures such as beam oscillators. Molecular dynamics simulation reveals that internal friction Q^{-1} in the carbon nanotube beam oscillators can be fitted with $T^{0.36}$ [36]. This is compared with a linear temperature dependence of Q^{-1} observed in crystalline, micromechanical resonators [37] and explained by assuming a reasonable density of defects within a linear

response theory of two-level systems [38, 39]. The dependence of quantum mechanical friction on temperature in micromechanical resonators has also been considered recently [40].

For s =27.5 Å, the post-wavy-motion frictional force per atom estimated from t =500 ps to 1 ns retains the same order of magnitude for all temperatures from 0 to 180 K despite its strong temperature dependence in the early phase of oscillation as shown in figure 11. This can be understood as follows. For zero temperature, as discussed previously, the frictional behaviour is attributed mainly to the wavy motion of the outer tube. As the DWNT is heated prior to the simulation, random thermal agitation in the nanotubes may hinder translational motion, aggravating the frictional effect in the initial phase of the oscillation on one hand, but may also disrupt collective phenomena, such as the wavy motion, on the other hand. The combined effect of the pre-simulation DWNT heating, for the case of s = 27.5 Å, leaves the post-wavy-motion frictional force, estimated from t = 500 ps to 1 ns, insensitive to the initial DWNT temperature. This also points to the fact that the intratube phonons responsible for frictional effects in the oscillator are most likely of low energies, and are saturated for s = 27.5 Å after the disappearance of the wavy motion. We conclude that pre-simulation heating of the DWNT oscillator increases the frictional force monotonically in the absence of the wavy motion, and such a picture obviously fails when the wavy motion plays an important role in the energy-transfer process.

6. Discussion

Via molecular dynamics in a micro-canonical ensemble, investigations are carried out on mechanisms of energy transfer from the orderly intertube translational oscillation to intratube vibrational modes for an isolated system of coaxial double-walled carbon nanotubes. Two novel energy dissipation mechanisms were identified which occur via collective motion of the nanotubes. For oscillators with 14.5 Å inner tubes, if a threshold of 2.1–2.6 meV/atom in excess intertube van der Waals energies is crossed, a form of rocking motion of the inner tube occurs upon re-entrance, and is responsible for significant intratube vibrational energy acquisitions. For oscillators with 55 Å inner tubes translational energies are predominately dissipated via a mechanism underlaid by the outershell wavy motion. The energy threshold for the occurrence of the wavy motion is 1.5–2.2 meV/atom. In the absence of the wavy motion, for example, by freezing the outershell atomic motion, dissipation via rocking motion is also found to occur above a certain energy threshold. Double-walled oscillators with one end-capped outershells as well as three-walled oscillators are also studied, and collisional reversals at the capped ends of the outer tube are found to provide additional energy dissipation. Doubling of the outershell mass does not appear to suppress the dissipative effect of the wavy motion in the three-walled oscillators with the inner tube extruded initially. Energetic instabilities of the concentric configuration upon middle-tube extrusion, however, render TWNT oscillators highly inefficient with respect to translational intertube movements. The dependence of the frictional behaviour on the pre-simulation DWNT temperature has also been investigated. In the absence of the wavy motion, the frictional force increases monotonically with the pre-simulation heating temperature of the nanotube oscillator, but such a picture fails when the initial extrusion length is large, and the wavy motion dominates the energy-transfer process. Simulation has been performed at different initial temperatures, revealing a strong temperature dependence of friction in the early phase of oscillation for an initial extrusion length s =27.5 Å. Pre-simulation heating, however, is found to disrupt collective modes such as the wavy motion,

and post-wavy-motion frictional behaviour appears insensitive to the heating temperature.

Coupled oscillator systems are often chosen in the literature for investigating energy exchange among various degrees of freedom, ergodicity on energy surfaces, and equipartition as systems relax. Fermi, Pasta, and Ulam reported the first numerical study on a chain of coupled oscillators with quartic anharmonicity in 1954, which is often referred to as the Fermi–Pasta–Ulam (FPU) model [41]. For a particular initial energy distribution it is observed that the oscillators do not relax to an equipartition state; instead, they display a persistent recurrence to the initial condition, contrary to the equipartition hypothesis of statistical mechanics. The dynamical behaviour of identical particles interacting via the Lennard-Jones potential has also been studied [42–44] with an aim to investigate the characteristics of the classical phase space of coupled oscillators, and their possible relevance to achieve nearly frictionless behaviour for sufficiently small solids. The nano-oscillators composed of two coaxial carbon nanotubes proposed by Zheng and Jiang [15] are in fact an extension of the one- and two-dimensional Lennard-Jones model to a practical three-dimensional construct with additional bonded interparticle interactions. This nanomachinery can therefore serve as a test bed for ergodicity and equipartition on complex energy surfaces.

The restoring forces for the DWNT nano-oscillator, which maximize at the positions of maximum extrusions, vary from 10^{-12} to 10^{-11} N/atom. This is compared with the frictional forces which are estimated to vary from 10^{-17} to 10^{-14} N/atom, depending on configurations and dissipative mechanisms. It is also interesting to compare various timescales in the nano-oscillator. The frequencies of translational oscillations long after the leap in acquired phonon kinetic energies are found to be about 140 GHz for the short-tube combination. For the long-tube combination, the frequencies are found to be approximately 40 GHz, which is much lower due to the longer length the inner tube must travel from one end to the other and its larger mass that has to be accelerated by a van der Waals force not dependent on the total length of the nanotube.

The Kolmogorov–Arnold–Moser (KAM) theory states that there exists a certain critical value of a small perturbation which determines the boundary of motion stability [45]. In general, the phase space of a classical system of coupled oscillators can be decomposed into regions of very different dynamical properties separated by boundaries corresponding to various energy thresholds. If the system energy is very close to the energy minimum, the KAM-like regime, ordered or quasiperiodic motion should be observed. For DWNT oscillators with short inner tubes, a regime of motion stability does exist for low system energies, and the onset of instability is initiated by misalignments of the inner tube axis with that of the outershell upon re-entrance. For oscillators with long inner tubes, motion stability exists for low energies as well, and instability is initiated by the outershell wavy motion underlaid by radial vibrations. On complex energy surfaces as is the case here, stochastic motion appears as the system energy is much higher than the minimum. We have found that the energy threshold (~2 meV/atom) for the DWNT oscillator to deviate from the KAM-like regime is not sensitive to the size of the system, in agreement with some earlier work on LennardJones chains [46]. This may be utilized in the design of nearly frictionless nano-mechanical devices.

Our findings here have several potential implications to the construction of nano-mechanical devices. For example, for low-energy applications, the KAM-like regime appears to be the ideal operating domain for DWNT oscillators. The simulations suggest that the

excess van der Waals energies per atom should be kept below about 2 meV in order to remain in the KAM-like regime for both long- and short-tube combinations. Significant intratube phonon energy acquisition is shown to occur via collective modes of the DWNT. In order to suppress the frictional effects, measures are to be taken to discourage excitation of those collective modes, such as to avoid significant extrusion of inner tube during oscillation, and to fix in space atoms in the outer tube so that the outer tube may appear more smooth to the intertube oscillation, i.e., free of dynamic roughness such as the wavy motion discussed in length here.

Acknowledgments

Support from the Hong Kong Research Grant Council (RGC), the US National Science Foundation (CMS-0140568), and the Committee for Research and Conference Grants (CRCG) of the University of Hong Kong, is gratefully acknowledged. One of the authors (YZ) would like to thank K Lindenberg for useful discussions.

References

[1] Iijima S 1991 *Nature* **354** 56

[2] Ebbesen T Wand Ajayan P M 1992 *Nature* **358** 220
Ebbesen T W*et al* 1993 *Chem. Phys. Lett.* **209** 83

[3] Iijima S and Ichihashi T 1993 *Nature* **363** 603

[4] Bethune D S *et al* 1993 *Nature* **363** 605

[5] White C T, Robertson D H and Mintmire J W 1993 *Phys. Rev.* B **47** 5485

[6] Saito R, Dresselhaus G and Dresselhaus M S 1998 *Physical Properties of Carbon Nanotubes* (London: Imperial College Press)

[7] Bockrath M *et al* 1997 *Science* **275** 1922

[8] Tsukagoshi K *et al* 1999 *Nature* **401** 572

[9] Antonov R D and Johnson A T 1999 *Phys. Rev. Lett.* **83** 3274

[10] Yao Z *et al* 1999 *Nature* **402** 273

[11] Tuzun R E, Noid D W and Sumpter B G 1995 *Nanotechnology* **6** 64

[12] Srivastava D 1997 *Nanotechnology* **8** 186
Bourlon B *et al* 2004 *Nano Lett.* **4** 709

[13] Cumings J and Zettl A 2000 *Science* **289** 602

[14] Berber S, Kwon Y K and Tománek D 2003 *Phys. Rev. Lett.* **91** 165503

[15] Zheng Q and Jiang Q 2002 *Phys. Rev. Lett.* **88** 045503
Zheng Q, Liu J Z and Jiang Q 2002 *Phys. Rev.* B **65** 245409

[16] Zhao Y, Ma C C, Chen G H and Jiang Q 2003 *Phys. Rev. Lett.* **91** 175504

[17] Legoas S B *et al* 2003 *Phys. Rev. Lett.* **90** 055504

[18] Rivera J L, McCabe C and Cummings P T 2003 *Nano Lett.* **3** 1001

[19] Guo W L *et al* 2003 *Phys. Rev. Lett.* **91** 125501

[20] Sapmaz S *et al* 2003 *Phys. Rev.* B **67** 235414

[21] Drexler K E 1992 *Nanosystems: Molecular Machinery, Manufacturing and Computation* (New York: Wiley) p 297

[22] Forro L 2000 *Science* **289** 560

[23] Carpick R W*et al* 1997 *Appl. Phys. Lett.* **70** 1548
Enachescu M *et al* 1998 *Phys. Rev. Lett.* **81** 1877

[24] Yu M F, Yakobson B I and Ruoff R S 2000 *J. Phys. Chem.* B **104** 8764

[25] Kolmogorov A N and Crespi V H 2000 *Phys. Rev. Lett.* **85** 4727

[26] Vuković T *et al* 2002 *Physica* E **16** 259

[27] Damnjanović M *et al* 2002 *Eur. Phys. J.* B **25** 131

[28] Lozovik Y E, Minogin A and Popov A M 2003 *Phys. Lett.* A **313** 112
Lozovik Y E, Minogin A and Popov A M 2003 *JETP Lett.* **77** 631

[29] Yu M-F, Lourie O, Dyer M J, Moloni K, Kelly T F and Ruoff R S 2000 *Science* **287** 637

[30] Huhtala M, Krasheninnikov A V, Aittoniemi J, Stuart S J, Nordlund K and Kaski K 2004 *Phys. Rev.* B **70** 045404

[31] Brooks B R, Bruccoleri R E, Olafson B D, States D J, Swaminathan S and Karplus M 1983 *J. Comput. Chem.* **4** 187

[32] Reigada R, Sarmiento A and Lindenberg K 2001 *Phys. Rev.* E **64** 066608

[33] Servantie J and Gaspard P 2003 *Phys. Rev. Lett.* **91** 185503

[34] Yoon J, Ru C Q and Mioduchowski A 2002 *Phys. Rev.* B **66** 233402

[35] Dubay O, Kresse G and Kuzmany H 2002 *Phys. Rev. Lett.* **88** 235506

[36] Jiang H, Yu M-F, Liu B and Huang Y 2004 *Phys. Rev. Lett.* **93** 185501

[37] Kleiman R N *et al* 1987 *Phys. Rev. Lett.* **59** 2079

[38] Phillips W A 1988 *Phys. Rev. Lett.* **61** 2632

[39] Keyes R W 1989 *Phys. Rev. Lett.* **62** 1324

[40] Ahn K H and Mohanty P 2003 *Phys. Rev. Lett.* **90** 085504

[41] Fermi E, Pasta J and Ulam S 1965 *Collected Papers of E. Fermi* ed E Segre (Chicago, IL: University of Chicago Press) p 978

[42] Benettin G*et al* 1980 *Phys. Rev.* A **22** 1709

[43] Sokoloff J B 1993 *Phys. Rev. Lett.* **71** 3450

[44] Sokoloff J B 1993 *Phys. Rev.* B **52** 7205

[45] Kolmogorov A N 1954 *Dokl. Akad. Nauk SSSR* **98** 527
Arnold V I 1963 *Russ. Math. Surv.* **18** 9
Moser J 1962 *Nachr. Akad. Wiss. Goett. Math.-Phys. K1.II* **1** 1

[46] Bocchieri P *et al* 1970 *Phys. Rev.* B **2** 2013

List of Table

List of Figures

Figure 9. (a) Calculated $K_{rel}(t)$ of a TWNT oscillator (70/70/55 Å) with the inner or middle tube extruded initially by a length s = 35 Å. Up to 500 ps of oscillational motion have been simulated.
(b) Centre-of-mass displacements of three nanotubes (solid, middle tube; dashed, inner tube; dotted, outer tube) along the translational direction when initially the middle tube is extruded.
(c) Centre-of-mass displacements of inner tube perpendicular to the translational direction when initially the middle tube is extruded.
(d) Centre-of-mass displacements of three nanotubes along the translational direction (solid, inner tube; dashed, middle tube; dotted, outer tube) when initially the inner tube is extruded.
(e) Centre-of-mass displacements of the inner tube perpendicular to the translational direction when initially the inner tube is extruded.

Figure 10. Intertube van der Waals energy as a function of the radial displacement D of the inner tube axis from its coaxial position in the absence of the middle tube. Configurational graphs are drawn for (a) the coaxial structure, D = 0 Å; (b) inner tube axis displaced by D = 3.0 Å from its coaxial position.

Figure 11. Relative displacement as a function of time for s = 27.5 Å and five different initial temperatures: 0, 60, 120, 180, 240 K.

Figure 12. Frictional force per atom (in 10^{-16} N/atom) as a function of pre-simulation heating temperature (in kelvin) for an initial extrusion length s = 7.5 Å. The temperature dependence can be fitted with $0.12T$ (in 10^{-16} N/atom) as shown by the solid line.

Table 1.

	Short DWNT		Long DWNT			TWNT
	One-end capped	Open-ended	One-end capped	Open-ended		Open-ended
Outer tube	18.5 Å (288)	14.5 Å (224)	74 Å (1056)	70 Å (992)	70 Å (992)	70 Å (1612)
Inner tube	14.5 Å (70)	14.5 Å (70)	55 Å (250)	14.5 Å (70)	55 Å (250)	55 Å (250)
Middle tube	—	—	—	—	—	70 Å (992)

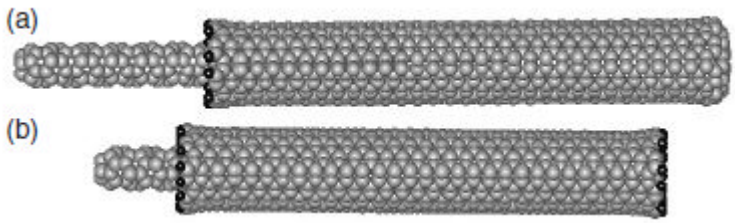

Fig. 1.

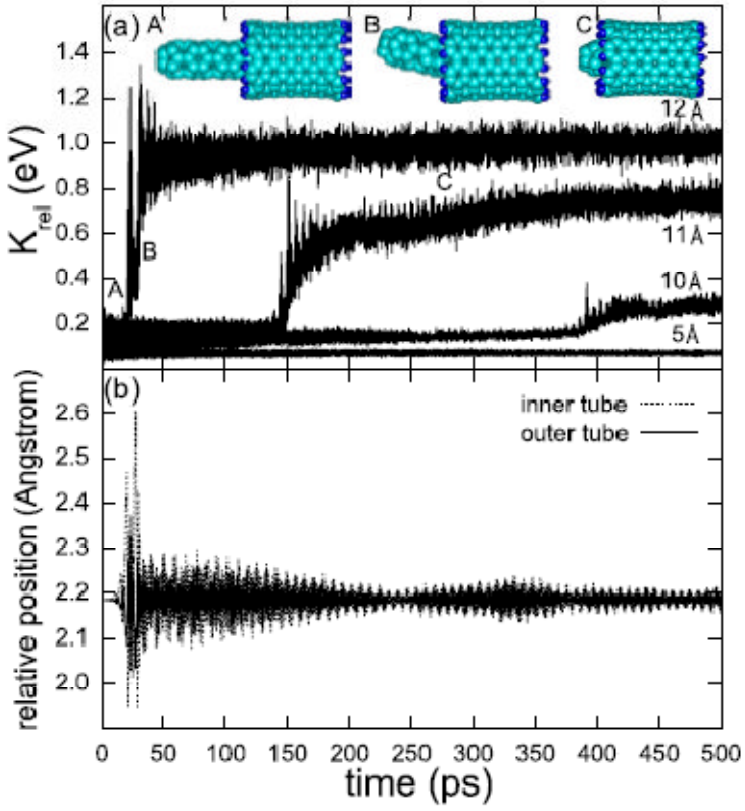
(a)
A
B
C
12Å
11Å
10Å
5Å
K_{rel} (eV)
1.4
1.2
1.0
0.8
0.6
0.4
0.2
(b)
inner tube
outer tube
relative position (Angstrom)
2.6
2.5
2.4
2.3
2.2
2.1
2.0
0
50
100
150
200
250
300
350
400
450
500
time (ps)

Fig. 2.

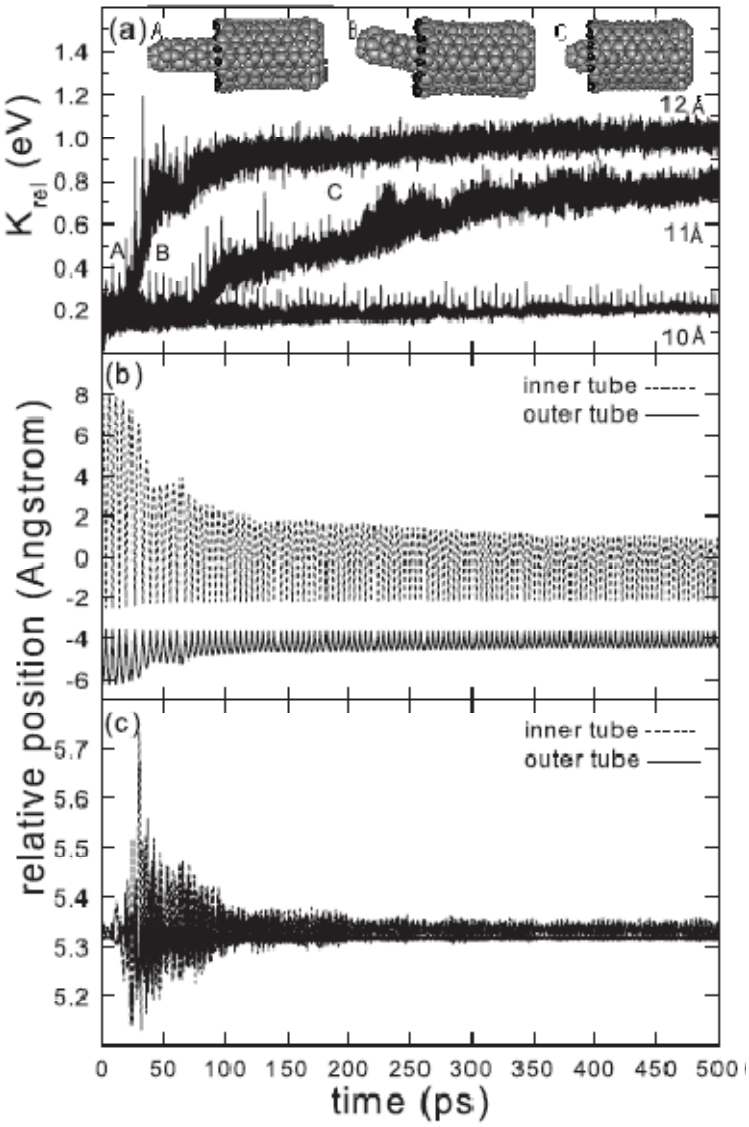
(a)
A
B
C
12Å
11Å
10Å
K_{rel} (eV)
(b)
inner tube
outer tube
(c)
inner tube
outer tube
relative position (Angstrom)
time (ps)

Fig. 3.

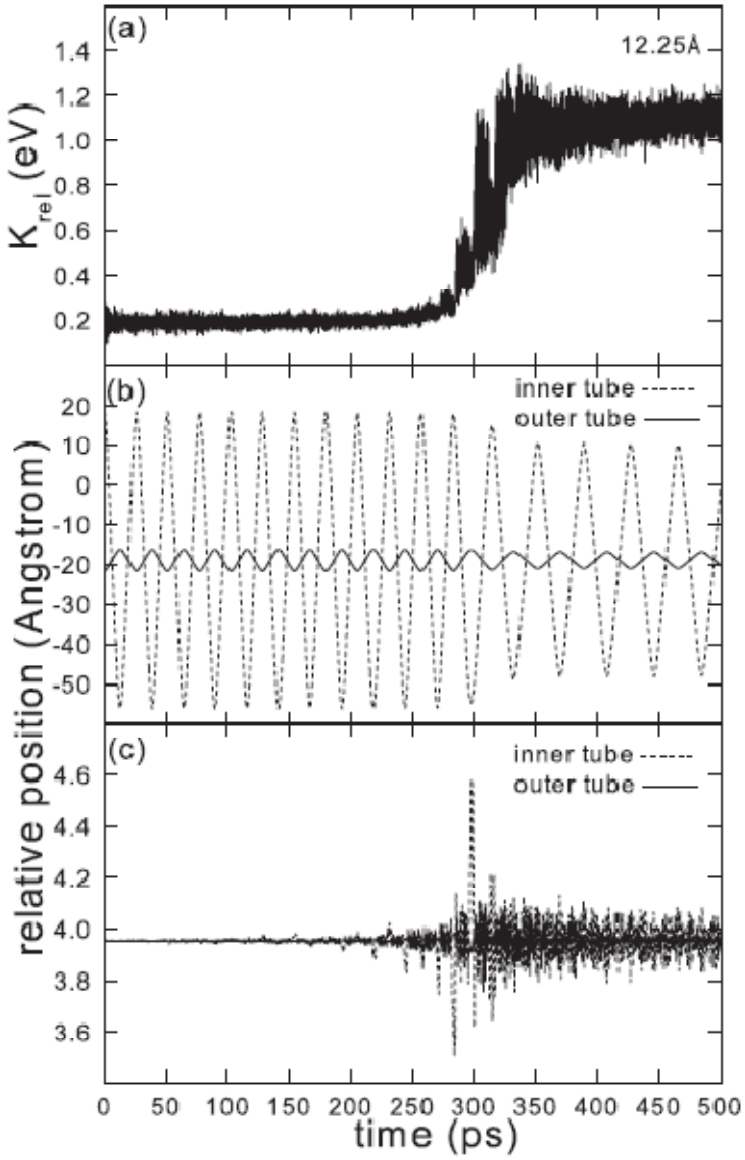
(a)
12.25Å
K_{rel} (eV)
1.4
1.2
1.0
0.8
0.6
0.4
0.2
(b)
inner tube
outer tube
20
10
0
-10
-20
-30
-40
-50
(c)
inner tube
outer tube
4.6
4.4
4.2
4.0
3.8
3.6
relative position (Angstrom)
0
50
100
150
200
250
300
350
400
450
500
time (ps)

Fig. 4.

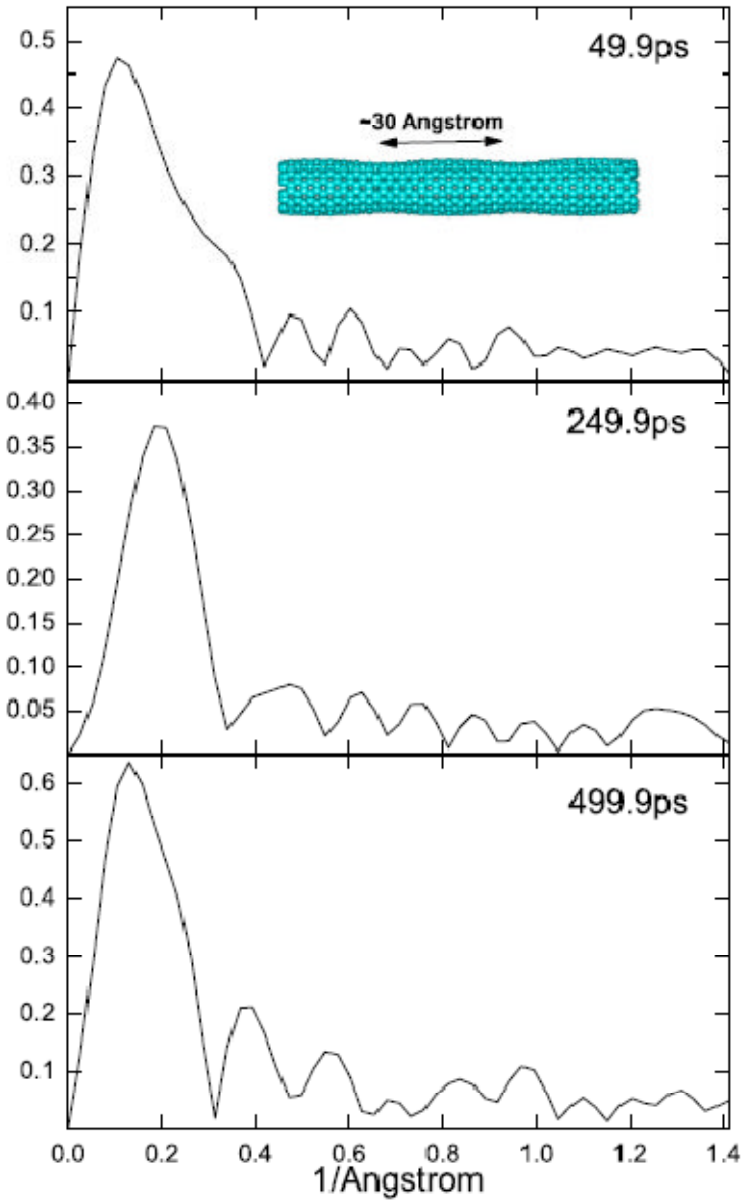
49.9ps
~30 Angstrom
249.9ps
499.9ps
0.5
0.4
0.3
0.2
0.1
0.40
0.35
0.30
0.25
0.20
0.15
0.10
0.05
0.6
0.5
0.4
0.3
0.2
0.1
0.0
0.2
0.4
0.6
0.8
1.0
1.2
1.4
1/Angstrom

Fig. 5.

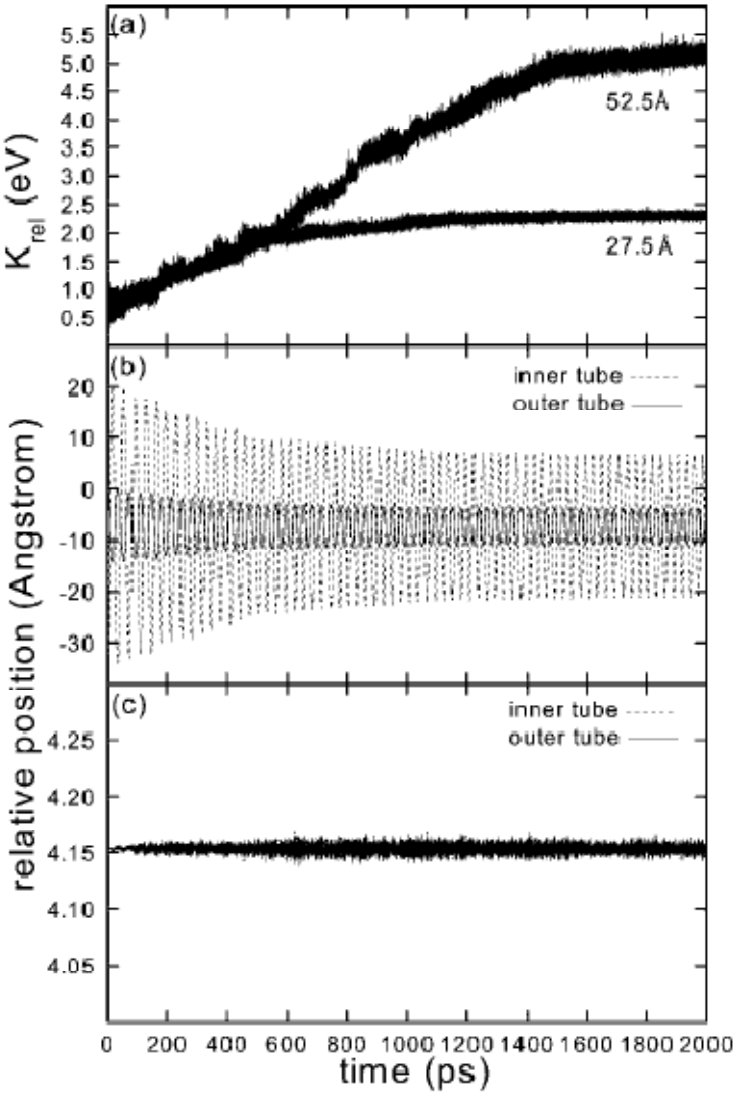
(a)
52.5Å
27.5Å
K_{rel} (eV)
(b)
inner tube
outer tube
(c)
inner tube
outer tube
relative position (Angstrom)
time (ps)

Fig. 6.

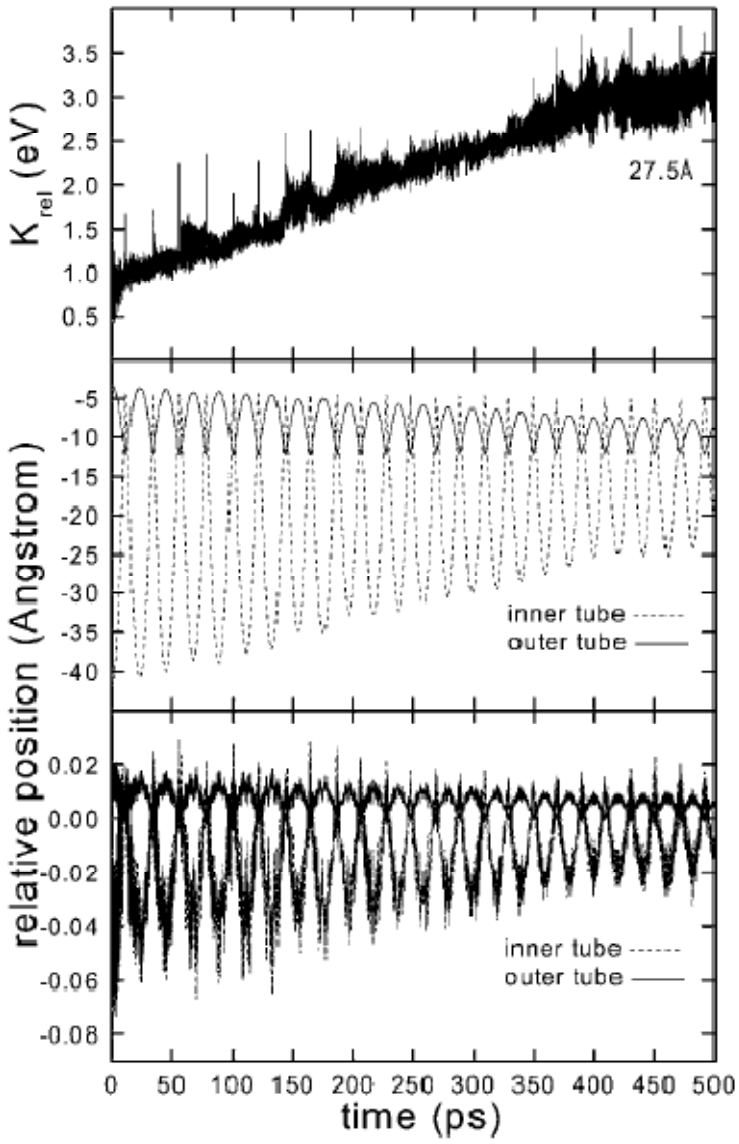
K_rel (eV)
3.5
3.0
2.5
2.0
1.5
1.0
0.5
27.5Å
relative position (Angstrom)
-5
-10
-15
-20
-25
-30
-35
-40
inner tube
outer tube
0.02
0.00
-0.02
-0.04
-0.06
-0.08
inner tube
outer tube
0
50
100
150
200
250
300
350
400
450
500
time (ps)

Fig. 7.

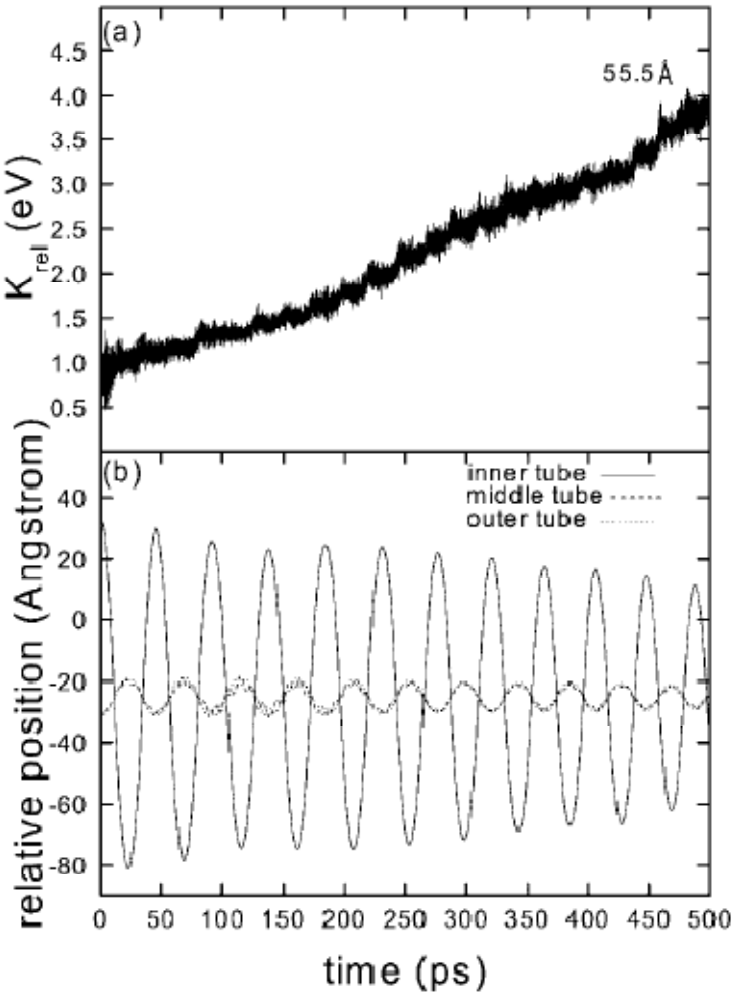
(a)
55.5Å
K_{rel} (eV)
4.5
4.0
3.5
3.0
2.5
2.0
1.5
1.0
0.5
(b)
inner tube
middle tube
outer tube
relative position (Angstrom)
40
20
0
-20
-40
-60
-80
0
50
100
150
200
250
300
350
400
450
500
time (ps)

Fig. 8.

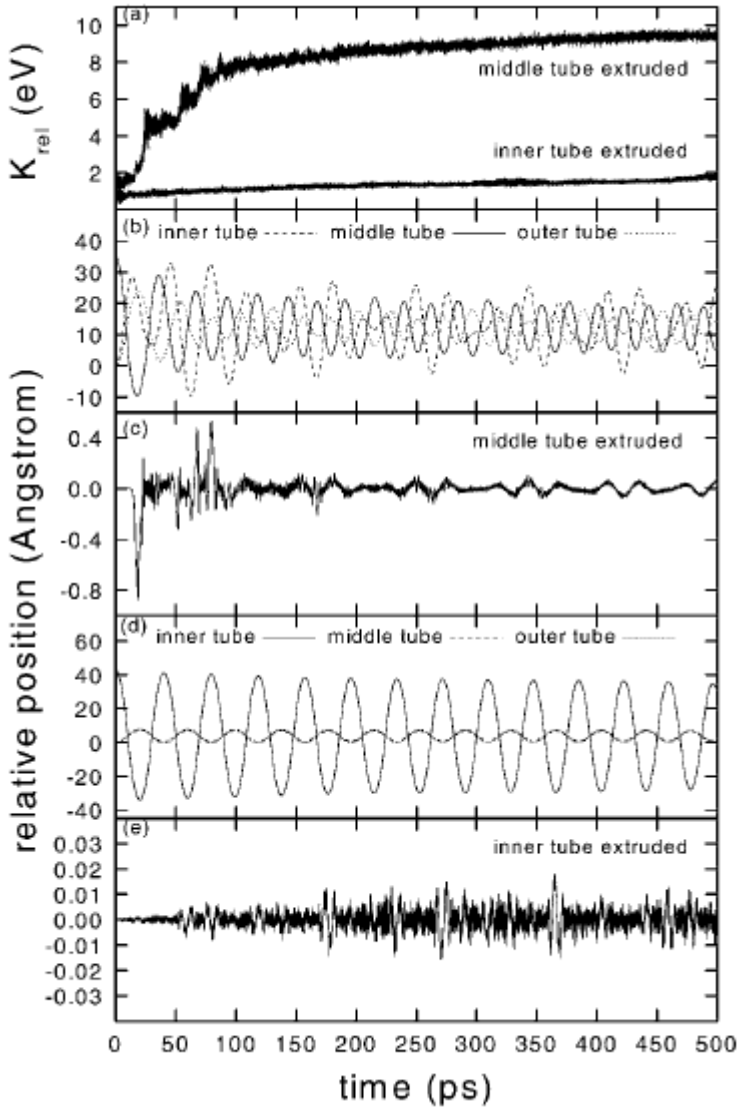
(a)
middle tube extruded
inner tube extruded
K_{rel} (eV)
(b) inner tube middle tube outer tube
(c) middle tube extruded
(d) inner tube middle tube outer tube
(e) inner tube extruded
relative position (Angstrom)
time (ps)

Fig. 9.

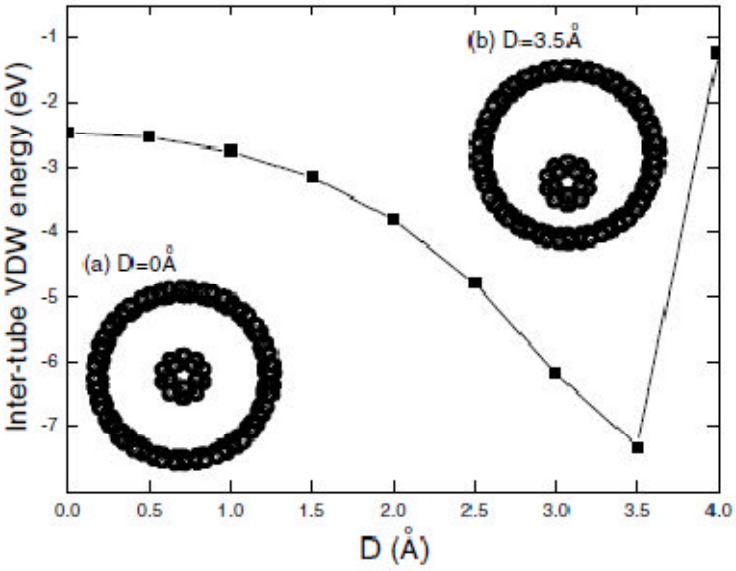
(b) D=3.5Å
(a) D=0Å
Inter-tube VDW energy (eV)
-1
-2
-3
-4
-5
-6
-7
0.0
0.5
1.0
1.5
2.0
2.5
3.0
3.5
4.0
D (Å)

Fig. 10.

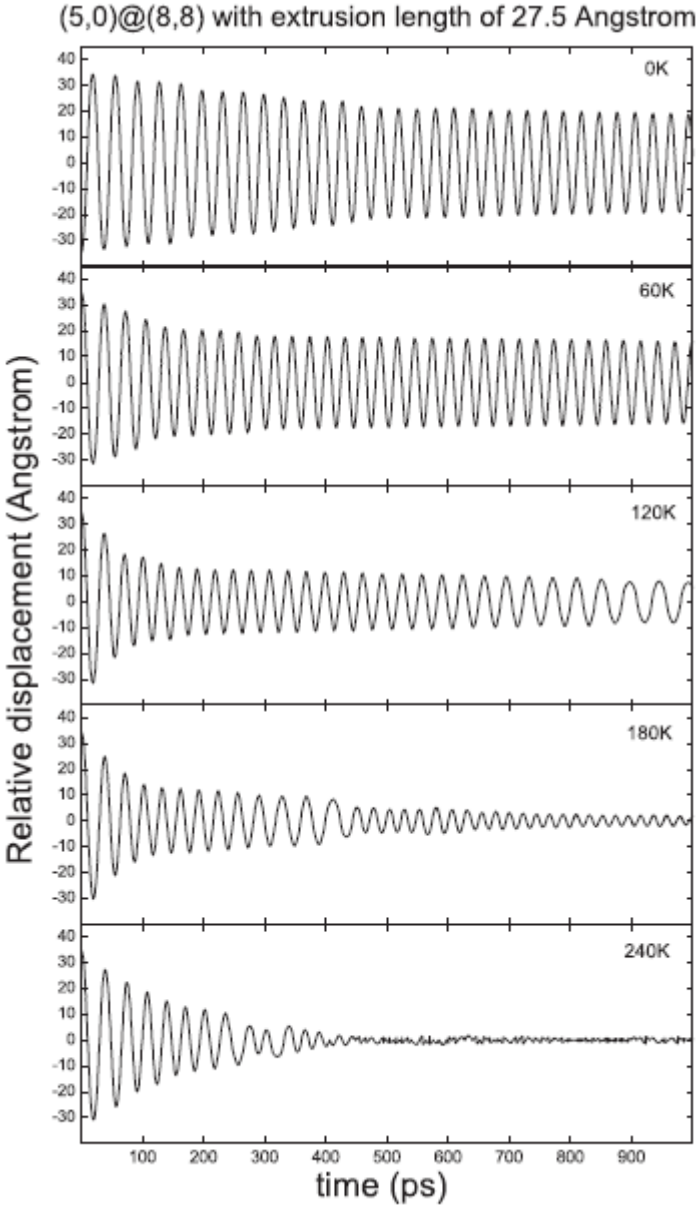
(5,0)@(8,8) with extrusion length of 27.5 Angstrom
0K
60K
120K
180K
240K
Relative displacement (Angstrom)
time (ps)

Fig. 11.

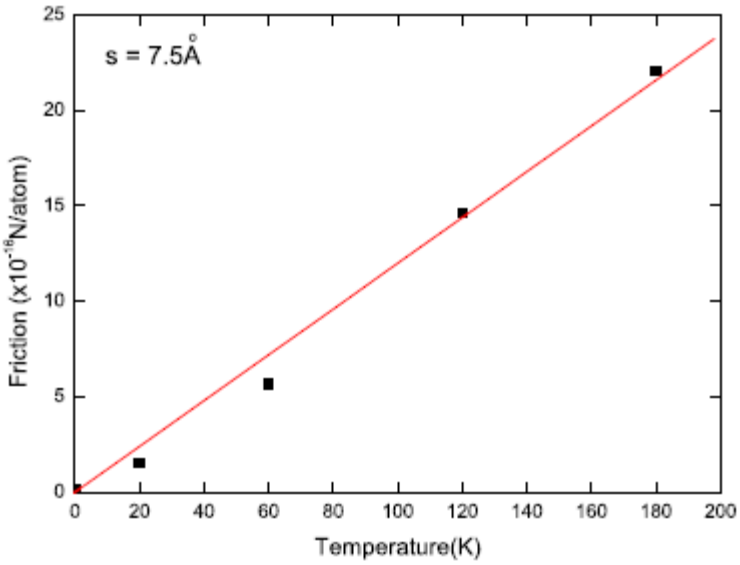
s = 7.5Å
Friction (x10^{-16}N/atom)
Temperature(K)
0
5
10
15
20
25
0
20
40
60
80
100
120
140
160
180
200

Fig. 12.